



Cite this: *Chem. Sci.*, 2024, **15**, 3907

All publication charges for this article have been paid for by the Royal Society of Chemistry

## Discovery of antibacterial manganese( $\text{I}$ ) tricarbonyl complexes through combinatorial chemistry†

Mirco Scaccaglia,<sup>1,2</sup> Michael P. Birbaumer,<sup>3</sup> Silvana Pinelli,<sup>3</sup> Giorgio Pelosi,<sup>1</sup> and Angelo Frei<sup>1\*</sup>

The continuous rise of antimicrobial resistance is a serious threat to human health and already causing hundreds of thousands of deaths each year. While natural products and synthetic organic small molecules have provided the majority of our current antibiotic arsenal, they are falling short in providing new drugs with novel modes of action able to treat multidrug resistant bacteria. Metal complexes have recently shown promising results as antimicrobial agents, but the number of studied compounds is still vanishingly small, making it difficult to identify promising compound classes or elucidate structure-activity relationships. To accelerate the pace of discovery we have applied a combinatorial chemistry approach to the synthesis of metalloantibiotics. Utilizing robust Schiff-base chemistry and combining 7 picolinaldehydes with 10 aniline derivatives, and 6 axial ligands, either imidazole/pyridine-based or solvent, we have prepared a library of 420 novel manganese tricarbonyl complexes. All compounds were evaluated for their antibacterial properties and 10 lead compounds were identified, re-synthesised and fully characterised. All 10 compounds showed high and broad activity against Gram-positive bacteria. The best manganese complex displayed low toxicity against human cells with a therapeutic index of  $>100$ . In initial mode of action studies, we show that it targets the bacterial membrane without inducing pore formation or depolarisation. Instead, it releases its carbon monoxide ligands around the membrane and inhibits the bacterial respiratory chain. This work demonstrates that large numbers of metal complexes can be accessed through combinatorial synthesis and evaluated for their antibacterial potential, allowing for the rapid identification of promising metalloantibiotic lead compounds.

Received 9th October 2023

Accepted 23rd January 2024

DOI: 10.1039/d3sc05326a

rsc.li/chemical-science

## Introduction

In 2019, over 1.3 million patients are estimated to have died from infections resistant to our current antibiotic arsenal.<sup>1</sup> Without urgent action and a strong replenishment of the antibiotic drug pipeline, the number of deaths is bound to increase further as antimicrobial resistance (AMR) is on the rise across the world. Unfortunately, the current clinical antibiotic candidates are both few in number and lacking in new targets, limiting their effective shelf-life from the start.<sup>2</sup> Over the last years, alternatives to the small organic molecule approaches to treat bacterial infections have increasingly been explored.<sup>3</sup> We have recently shown that transition metal complexes display promising antimicrobial properties. In a systematic study of

over 300 000 tested molecules by the Community for Open Antimicrobial Drug Discovery (CO-ADD), metal-containing compounds had a 10 $\times$  higher hit-rate against critical ESKAPE (*Enterococcus faecium*, *Staphylococcus aureus*, *Klebsiella pneumoniae*, *Acinetobacter baumannii*, *Pseudomonas aeruginosa*, and *Enterobacter* spp.) pathogens compared to regular organic molecules. Additionally, metal complexes did not show increased rates of cytotoxicity or haemolysis in this comparison.<sup>4</sup> In the last decade, a few key studies have investigated metal complexes for their antibacterial properties in-depth with several showing promising *in vitro* and *in vivo* activity.<sup>4–12</sup>

Amongst the only small number of metal compound classes studied for their antibacterial properties, the metal carbonyl core ( $\text{M}(\text{CO})_3$ ) is a commonly occurring motif. Patra *et al.* were the first to highlight that the antibacterial properties of a trimetallic metal compound could be attributed to the presence of a rhenium tricarbonyl moiety in the structure.<sup>13</sup> Mode of action studies attributed the activity of this compound to its detrimental effect on the bacterial cell membrane, causing depolarization but not pore formation. However, due to unfavorable solubility and cytotoxicity properties, the compounds were not evaluated further. More recently, several groups have investigated metal complexes based on the  $\text{Re}(\text{CO})_3$ -scaffold. Frei *et al.*

<sup>1</sup>Department of Chemistry, Life Sciences and Environmental Sustainability, University of Parma, 43124 Parma, Italy

<sup>2</sup>Department of Medicine and Surgery, University of Parma, Via Gramsci 14, 43126 Parma, Italy

<sup>3</sup>Department of Chemistry, Biochemistry & Pharmaceutical Sciences, University of Bern, Freiestrasse 3, 3012 Bern, Switzerland. E-mail: angelo.frei@unibern.ch

† Electronic supplementary information (ESI) available. CCDC 2280008–2280010.

For ESI and crystallographic data in CIF or other electronic format see DOI: <https://doi.org/10.1039/d3sc05326a>



reported on dual-mode of action bisquinoline rhenium tricarbonyl complexes which exhibited both light dependent and independent antibacterial activity against drug-resistant Gram-positive and Gram-negative bacteria.<sup>14</sup> The group of Zobi has shown that *fac*-[Re(CO)<sub>3</sub>] diimine compounds display activity against Gram-positive bacteria, including drug-resistant ones. The complexes were further shown to be effective in a zebrafish infection model.<sup>15,16</sup>

Manganese, the first-row transition metal congener of rhenium, has also been explored by several groups for its antibacterial properties. Due to the higher lability of the carbonyl ligands, manganese tricarbonyl complexes have been studied extensively as CO-releasing molecules (CORMs). Mendes *et al.* have synthesised and studied a series of manganese and rhenium tricarbonyl compounds bearing the antifungal drug clotrimazole as an axial ligand. A detailed study of one rhenium complex suggests that part of its mode of action involves inhibition of peptidoglycan synthesis in Gram-positive bacteria by coordinating to lipid I, lipid II and undecaprenyl-pyrophosphate C55PP.<sup>17</sup> The group of Schatzschneider has first reported the antimicrobial activity of a manganese based light-activated CORM (photocORM) in 2014.<sup>18</sup> This complex and related ones have been extensively studied for their antimicrobial properties in the last decade.<sup>19–22</sup> The same group also described Mn(CO)<sub>3</sub> compounds with light independent antibacterial effects *in vitro* and *in vivo*.<sup>23–25</sup> Ward *et al.* reported a tryptophane-based Mn(CO)<sub>3</sub> photocORM which showed good antibacterial activity against *N. gonorrhoeae* and *S. aureus* upon light irradiation.<sup>26,27</sup> A water-soluble Mn(CO)<sub>4</sub>-based CORM (CORM-401) was first highlighted by Crook *et al.* and its antimicrobial

properties were studied by Wareham *et al.*<sup>28,29</sup> The group showed that CORM-401 does not inhibit respiration, but instead disrupts the cytoplasmic ion balance and induces, amongst other effects, osmotic stress. Of note, the antimicrobial effects were only found at high compound concentrations and toxicity against eukaryotic cells was observed.<sup>29</sup>

While the potential of metal complexes and the metal-carbonyl scaffold in particular has clearly been established in recent years, current approaches usually focus on the investigation of only a handful of compounds at a time. This makes the exploration of this compound class inefficient as well as time- and resource-intensive. Additionally, while promising molecules have been found, very little is understood about the structure-activity relationships amongst them.

Combinatorial synthesis has been applied successfully in conventional medicinal chemistry to efficiently explore the organic chemical space for promising compounds.<sup>30</sup> In particular its combination with DNA-encoded chemical libraries has led to several lead-compounds that have advanced to clinical trials.<sup>31</sup> The combinatorial concept has been applied to the synthesis of metal complexes as well, albeit only in a limited number of examples. The group of Bernhard has utilised various permutations of bidentate N<sup>+</sup>N and C<sup>+</sup>N-type ligands to prepare large libraries of iridium complexes with promising photophysical properties.<sup>32–34</sup> The group of Schatzschneider has recently reported the application of so-called iClick reactions to combinatorially prepare [Ru(triazolato)(N<sup>+</sup>N)(terpy)]PF<sub>6</sub> complexes.<sup>35</sup>

In the context of medicinally applied combinatorial metal complex synthesis, the group of Ang has pioneered a three-component assembly (3CA) protocol for the synthesis of

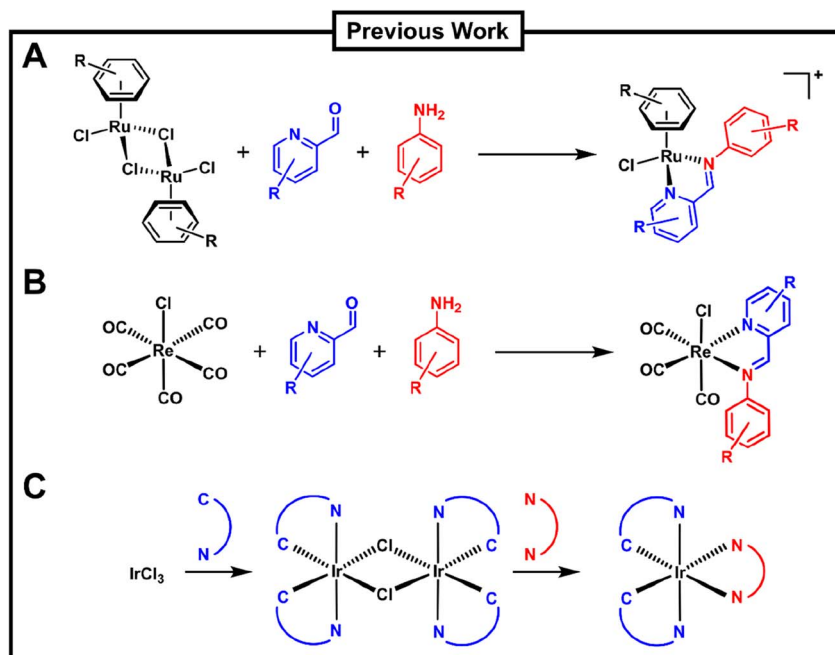


Fig. 1 Overview of previous work on the combinatorial synthesis of metal complexes which included biological evaluation of the prepared compounds by the groups of (A) Ang, (B) Wilson and (C) Vilar.



Schiff-base arene ruthenium(II) complexes (Fig. 1A).<sup>36</sup> The group utilised different ruthenium arene precursors in combination with robust Schiff-base ligands formed by the combination of different picolinaldehydes with aniline derivatives to form stable piano-stool type complexes under mild conditions. This approach has been applied to synthesize hundreds of different ruthenium complexes and explore their anticancer, antibacterial and catalytic properties.<sup>37–40</sup> Konkankit *et al.* have applied a similar approach, albeit only with two components, to the preparation of rhenium carbonyl complexes, identifying some with potent anticancer properties (Fig. 1B).<sup>41,42</sup> Very recently Kench *et al.* reported an approach similar to the Bernhard group for the preparation of polypyridyl iridium complexes. However, in this case the workflow was optimised to obtain photocytotoxic compounds with activity against human cancer cells (Fig. 1C).<sup>43</sup>

In light of the promising antibacterial properties reported for carbonyl and specifically manganese tricarbonyl complexes, we have adapted the combinatorial chemistry approach to the systematic synthesis of these compounds. Herein we report the rapid, efficient and economical synthesis of 420 novel manganese tricarbonyl Schiff-base compounds. The complexes were characterised and explored for their antibacterial properties and toxicity. We identified and re-synthesised 10 lead complexes which were isolated and fully characterised. These compounds were further studied for their physicochemical properties and extended biological studies were conducted.

## Results and discussion

### Optimization of $\text{MnCO}_3$ combinatorial synthesis and preparation of compound library

For a reaction protocol to be applicable to combinatorial chemistry, the conditions need to (a) be sufficiently robust to tolerate a variety of building blocks and (b) be adaptable to a relatively high throughput set up. We chose  $[\text{MnBr}(\text{CO})_5]$  as our starting material due to its commercial availability and its established use as a precursor to  $\text{Mn}(\text{CO})_3$  type compounds. The formation of Schiff-base type ligands starting from picolinaldehydes and aniline derivatives has proven a promising strategy as the reaction occurs under mild conditions and in a variety of solvents, including water.<sup>36,41</sup> In order to add a third dimension to the diversity of synthesised compounds, we introduced an axial ligand to the third available coordination site (Fig. 2).

Initial reaction attempts starting directly from  $[\text{MnBr}(\text{CO})_5]$  gave low conversion rates and required long reaction times as well as high temperatures as determined by LC-MS. Through extensive screening of reaction conditions, we determined that a pre-activation of the  $[\text{MnBr}(\text{CO})_5]$  precursor by reaction with one equivalent of silver triflate under inert atmosphere and in dry THF led to a more reactive intermediate. This ‘solvated’ manganese tricarbonyl could be directly utilised for further reaction with the Schiff-base components and the axial ligand in one pot, requiring only 90 min heating at 70 °C under ambient atmosphere. Initially, the reactions were attempted in

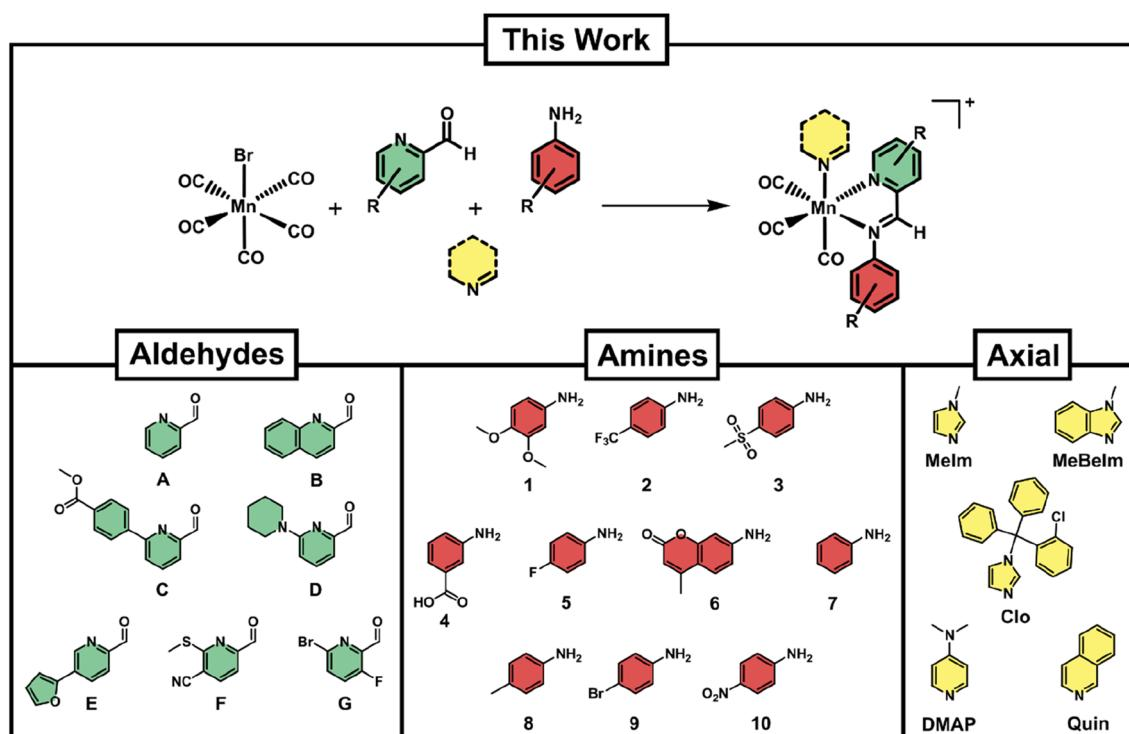


Fig. 2 General reaction scheme of the combinatorial synthesis of manganese tricarbonyl Schiff-base complexes and overview of chemical building blocks selected for the synthesis of 420 novel complexes (all 70 possible Schiff-base complexes where also synthesised without the addition of the N-donor axial ligand, likely leading to the coordination of a solvent molecule).



DMSO and DMSO/H<sub>2</sub>O mixtures to enable direct biological screening of the reaction crudes. However, the conversion rates in these solvents were not satisfactory. Eventually, it was found that THF provided the best compromise of good conversion rates and ease of removal after reaction completion.

Several considerations went into the selection of picolinaldehyde, aniline and axial ligand building blocks. A list of commercially available picolinaldehyde derivatives was obtained from the Reaxys platform. These compounds were further filtered by price and their chemical similarity was determined by Tanimoto indices.<sup>44</sup> Seven picolinaldehydes with maximised diversity and reasonable price were eventually obtained (Fig. 2). In the case of anilines, a large number of these structures were available in our department. From these, a set of 10 maximally diverse (based on their Tanimoto similarity) were chosen for our library. Lastly, several compounds were screened as axial ligands in test-reactions, revealing that even with optimised conditions some axial ligands did not lead to sufficiently high conversion rates. The final selection of axial ligands (Fig. 2) is hence a subset of the ones that were coordinating successfully under our reaction conditions. The antifungal clotrimazole (**Clo**) has been utilised as a ligand in several other studies and found to convey some level of biological activity that goes beyond the activity of the parent compound.<sup>17,22,45</sup> We have hence included it in our studies as a means to compare our compounds to others reported in the literature.

With the 10 anilines, 7 picolinaldehydes and 5 N-donor axial ligands in hand we proceeded to set up the combinatorial syntheses. As a control, we conducted the reaction without the addition of the N-donor axial ligand, likely leading to the coordination of a solvent molecule at the axial side of the compounds. Briefly, 70 reactions at a time were set up by combining equimolar amounts of pre-activated manganese carbonyl (20 mM, 100 µL) together with the different building

blocks from pre-prepared stock solutions in THF (40 mM, 50 µL) in 500 µL polypropylene tubes. The reaction vessels were sealed and heated in the dark for 90 min. The solvent was then removed *in vacuo* and the dried reaction crudes re-dissolved in 100 µL of DMSO (stock solution 20 mM) and diluted in acetonitrile for LC-MS analysis. The LC-MS spectra were analyzed for both target product formation and conversion percentage (a representative sample of LC-MS spectra are given in the ESI, Fig. S1†). Altogether 420 novel manganese complexes could be prepared and characterised by LC-MS with minimal use of reagents (less than 1 mg bromopentacarbonylmanganese per reaction).

### Antimicrobial activity of combinatorial Mn(CO)<sub>3</sub> library

To efficiently get a picture of the antibacterial activity profile of all 420 compounds we conducted a single-concentration screen of all crude reaction mixtures at 100 µM against the Gram-positive methicillin resistant *S. aureus* (MRSA) and the Gram-negative *Escherichia coli*. For compounds that showed complete growth inhibition under these conditions, we conducted a microdilution dose response assay to determine a minimum inhibitory concentration (Fig. 3 and Table S1†).

Firstly, in line with most tricarbonyl complexes reported in the literature, barely any activity was observed against the Gram-negative *E. coli*. While 38 compounds showed some inhibition in the single concentration assay at 100 µM, an MIC could only be determined for 5 compounds. The lowest determined MIC was 50 µM for **MnA7Clo**. Conversely much higher levels of activity were detected against the Gram-positive MRSA. Of all 420 compound crudes tested, an MIC could be determined for 152 (36.2%) of them (Fig. S2†). Only for 31 compounds where growth inhibition was observed in the single concentration assay at 100 µM no MIC could be detected at that or lower concentrations. If an active compound is defined to have an

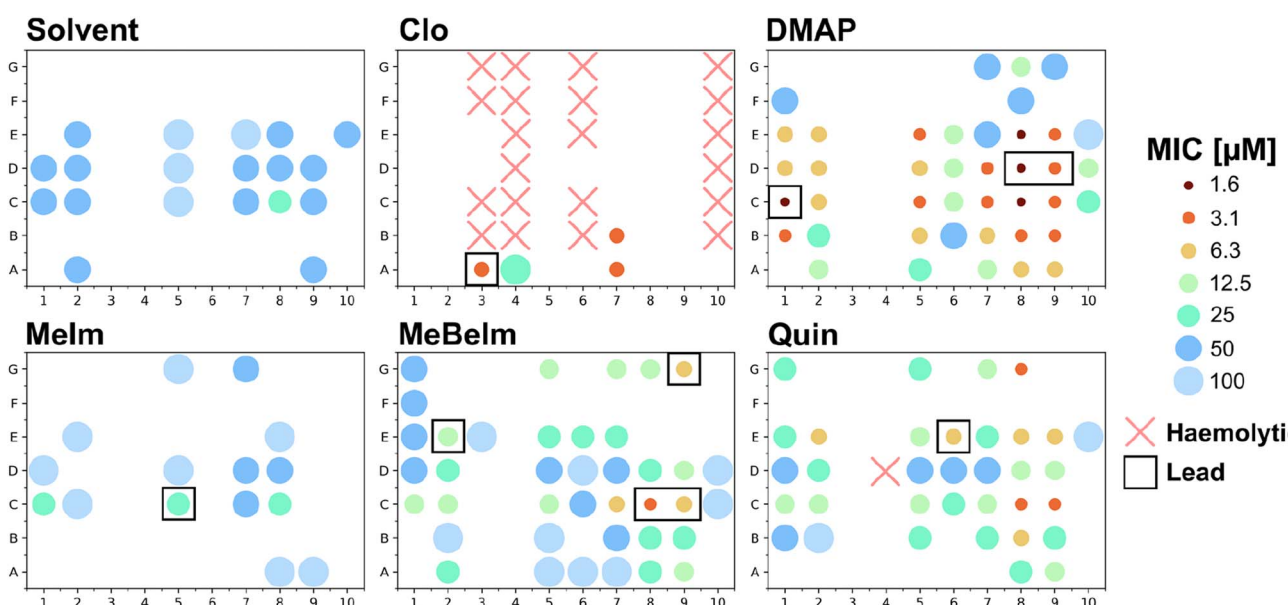


Fig. 3 Overview of antibacterial activity of the 420 combinatorial manganese complexes against methicillin resistant *Staphylococcus aureus* COL (MRSA). Haemolytic properties are also indicated and the 10 selected lead compounds are highlighted.



MIC of 12.5  $\mu\text{M}$  or lower, 64 of the 420 compounds (15.3%) would classify as active. A notable 39 (9.3%) had an MIC of 6.25  $\mu\text{M}$  or lower and for four an MIC of 1.56  $\mu\text{M}$  was found. To verify if the observed activity could stem from the building blocks instead of the complex, we also tested all picolinaldehydes, anilines and axial ligands. No activity was observed for any of the building blocks except for **Clo** which showed an MIC of 12.5  $\mu\text{M}$  against MRSA (Table S2†), confirming that in most cases the observed activity is likely due to the formed manganese tricarbonyl complex. Significantly more active compounds are observed with the **MeBeIm**, **DMAP** and **Quin** axial ligands. Among the picolinaldehydes building blocks we observe that 65% of all actives (*i.e.* MIC  $\leq$  12.5  $\mu\text{M}$ ) contain one of the bicyclic picolinaldehydes *i.e.* **C**, **D** or **E**. On the other hand for the anilines, polar (**3**, **4** and **10**) and/or bulky (**6**) derivatives seemed to be unfavorable for antibacterial activity.

Overall, this hit-rate is impressive yet not entirely unsurprising, considering the literature precedent on this compound class. To obtain a first indication on the potential toxicity of the synthesised complexes against human cells, we also tested all 420 crudes for haemolytic properties against human red blood cells. Only 22 compounds, 21 of which contained the **Clo** axial ligand, showed any sign of haemolysis at 20  $\mu\text{M}$  (Fig. 3). Additionally, all compounds that displayed hemolysis in this assay did not have any antibacterial activity. Overall, this first toxicity screening indicates that the majority of these manganese Schiff-base compounds are non-haemolytic.

So far, all tested substances were reaction crudes containing the target compound with an average purity of  $64 \pm 14\%$ . All

assays so far were conducted with non-purified compounds to enable a significantly higher throughput in much less time. However, the ambiguous purity of the crudes leaves open the possibility that the observed activity could be due to side products or impurities instead of the putative metal complex.

### Resynthesis, purification and characterisation of lead compounds

After the preliminary biological assessment, we selected ten lead compounds for resynthesis (Fig. 4). The selection of lead compounds was based on the determined antibacterial activity. Additionally, we aimed to maximize the chemical diversity of the lead compounds, aiming to have at least one example with each axial ligand included. The selected compounds were resynthesised *via* conventional batch-style chemistry on a  $\sim$ 20 mg per 72  $\mu\text{mol}$  scale and purified by preparative HPLC with yields ranging from 26–99% (in some cases the pure compound could be isolated directly by precipitation). The pure metal complexes were characterised by  $^1\text{H}$  and  $^{13}\text{C}$  NMR, LC-MS, HR-MS and IR spectroscopy (see ESI†). Single crystals suitable for X-ray diffraction structural elucidation were obtained for compounds **MnD8DMAP**, **MnC1DMAP**, and **MnG9MeBeIm** (Fig. 5).

The X-ray structures of these compounds introduce an unexplored family of molecules in the CSD database. Structural analysis unveils the manganese atom's adoption of a pseudo-pentahedral configuration, wherein a *fac*- $\text{Mn}(\text{CO})_3$  moiety coordinates the bidentate Schiff-base and the N-donor axial ligand sourced from either imidazole or pyridine. Notably, bond

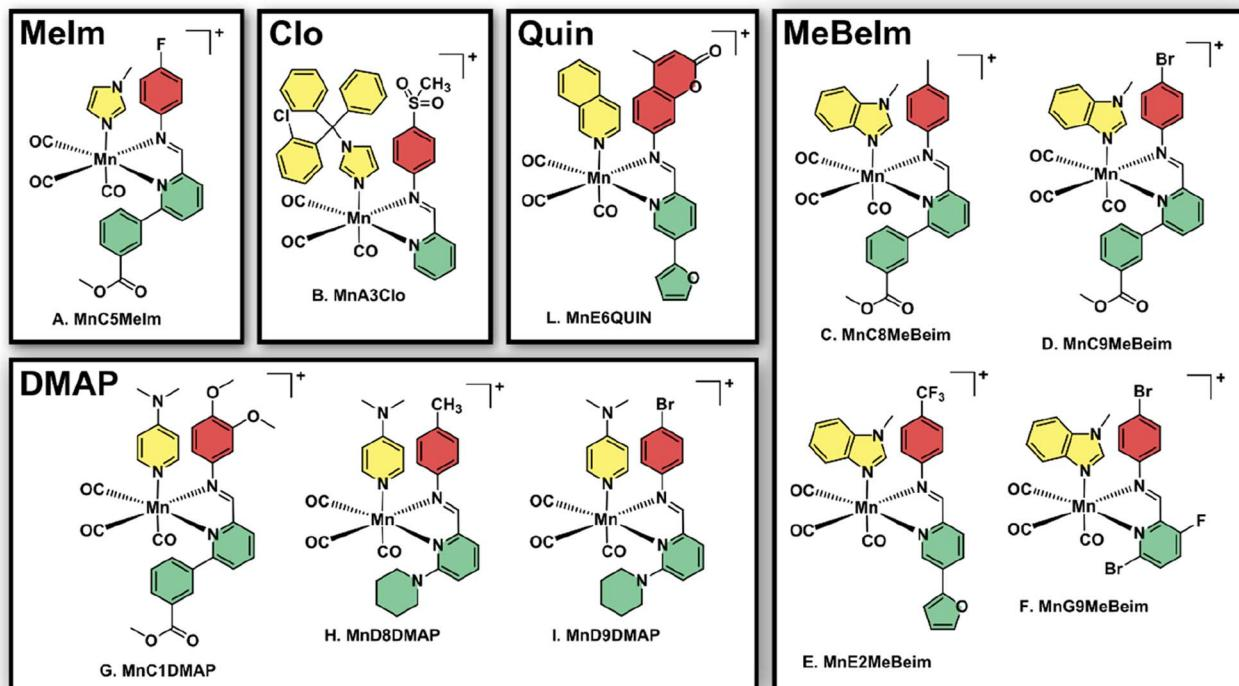


Fig. 4 Structures of the 10 manganese lead compounds that were re-synthesised, purified and characterised after the initial combinatorial screening campaign. Counterion (either TFA or triflate *cf.* ESI†) is omitted for clarity.



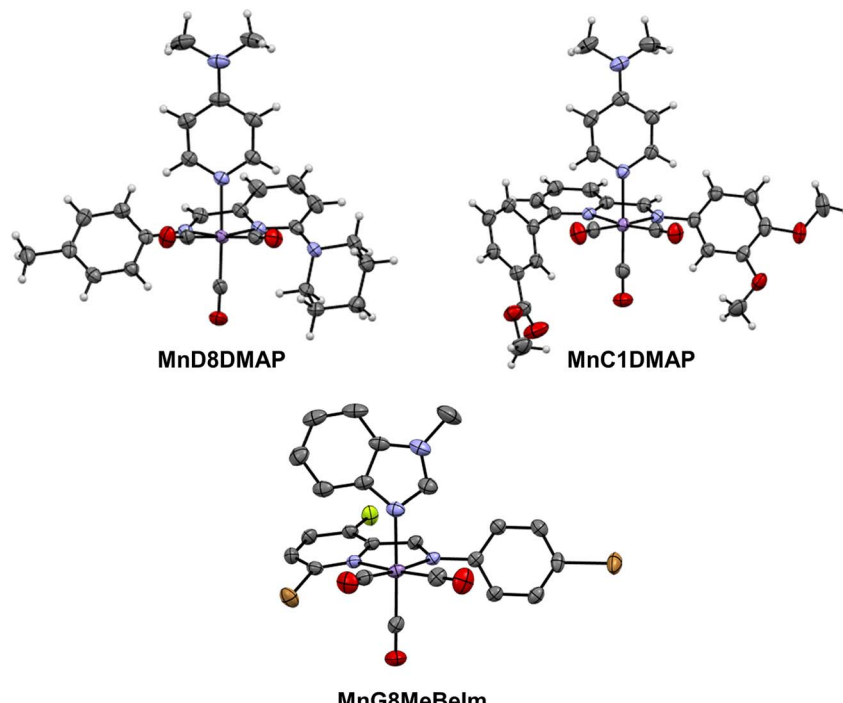


Fig. 5 Molecular structure of the cationic moieties of **MnD8DMAP**, **MnC1DMAP** and **MnG9MeBelM** (CCDC No 2280008-10). Atomic displacement ellipsoids are shown at the 50% probability level. The triflate counterion and a co-crystallised solvent molecule are omitted for clarity. Color coding: carbon (grey), hydrogen (white), nitrogen (blue), oxygen (red), bromine (orange), manganese (purple).

distances (as detailed in Table S3†) exhibit minimal differences across the three structures in this study, aligning with expectations from the parent compounds.<sup>46</sup> Interestingly, the Schiff-base's two rings remarkably deviate from planarity, with unusually large dihedral angles spanning between 37° and 46°.

#### Biological valuation of the lead manganese compounds

With the pure lead compounds in hand, we conducted anti-bacterial activity assays against a selection of Gram-positive and Gram-negative bacteria (Tables 1 and S4†). The compounds showed generally good activity against a variety of strains, including the ESKAPE pathogens MRSA and vancomycin resistant *Enterococcus* clinical isolate strains. Some of the compounds showed moderate activity against the Gram-negative *A. baumannii* and *E. coli* indicating that further structural optimisation might lead to a compound with broad spectrum antibacterial activity (Table S4†). To ascertain whether the lead compounds are bacteriostatic or bactericidal the minimum bactericidal concentration (MBC) was determined against MRSA (Table S5†). For all compounds except **MnC5MeBelM**, the MBC was found to be very close to the MIC, suggesting that most of the tested compounds are bactericidal.

To further evaluate the potential toxicity of the lead compounds, we re-measured haemolysis, determining  $HC_{50}$  values and tested them for cytotoxicity against eukaryotic healthy human epithelial cells (HuDe). Overall, the activity observed for the crude reaction mixtures translated to activity for the pure compound with high fidelity, validating the combinatorial chemistry approach for the discovery of antibacterial metal

complexes pursued in this project. Similarly, the haemolysis values determined with the pure compounds are in agreement with the measurements for the crudes *i.e.* no compound shows haemolysis under 49  $\mu$ M. On the other hand, relatively high levels of cytotoxicity against HuDe cells were observed for some of the compounds. Nevertheless, three of the lead compounds still displayed therapeutic indices (TI) of  $>10$  with **MnG9MeBelM** having a TI of  $>100$ . Notably this compound contains two bromide substituents in its bidentate ligand which account for a quarter of the compounds molecular weight, indicating that heavy halogen substituents could be important for the observed properties. The MICs of **MnG9MeBelM** were comparable to the standard of care for Gram-positive infections, vancomycin (VAN).

As already mentioned, some manganese tricarbonyl complexes are known for their light-mediated carbon monoxide release. Indeed, we observed rapid decomposition of these compounds when exposed to natural daylight as evidenced by decolorisation of stock solutions. However, no such decolorisation was observed under dim-light conditions, and reproducible data was obtained across multiple biological and technical replicates. To further study the stability of these compounds, we measured their UV/vis absorbance in different solvents (water, DMSO, HEPES, PBS) over time to see if any changes were visible (Fig. S3–S12†). Over an 18 hours period, no decomposition was observed in DMSO and only small changes in absorbance were detected in water and the buffers.

Based on these extensive biological data, compound **MnG9MeBelM** was chosen as the sole lead compound for further studies due to its high level of antibacterial activity



**Table 1** Antibacterial activity against a selection of Gram-positive strains, toxicity data in HuDe cells and human red blood cells and therapeutic indices (TI) for the 10 synthesised lead compounds<sup>a</sup>

	MIC [ $\mu$ M] vs. Gram-positive bacteria						Toxicity [ $\mu$ M]		
	MRSA	MSSA	Se	Bs	En	En VRE	CC <sub>50</sub>	HC <sub>50</sub>	TI
<b>MnC5MeIm</b>	3.13–6.25	12.5–6.25	12.5	12.5–6.25	25	25	46.1 $\pm$ 0.1	>200	7
<b>MnA3Clo</b>	1.56	1.56	3.13	3.13–1.56	6.25	3.13	37.1 $\pm$ 0.2	68 $\pm$ 15	24
<b>MnC8MeBeIm</b>	3.13–1.56	6.25	6.25	6.25	12.5	6.25	18.0 $\pm$ 0.2	77 $\pm$ 10	6
<b>MnC9MeBeIm</b>	3.13–1.56	3.13	6.25	3.13	12.5	12.5	16.8 $\pm$ 0.2	95 $\pm$ 13	5
<b>MnE2MeBeIm</b>	3.13–1.56	3.13	6.25–3.13	3.13	12.5	12.5	7.2 $\pm$ 0.3	49 $\pm$ 12	2
<b>MnG9MeBeIm</b>	0.78	<0.78	<0.78	3.13–1.56	6.25	6.25	85.2 $\pm$ 0.1	117 $\pm$ 12	109
<b>MnC1DMAP</b>	3.13–1.56	3.13–1.56	6.25	6.25–3.13	12.5	6.25	37.0 $\pm$ 0.2	>200	12
<b>MnD8DMAP</b>	1.56	1.56–0.78	1.56	3.13–1.56	12.5	12.5	7.9 $\pm$ 0.2	>200	5
<b>MnD9DMAP</b>	1.56	1.56	3.13	1.56	12.5	6.25	9.4 $\pm$ 0.2	>200	6
<b>MnE6Quin</b>	6.25–3.13	6.25	12.5–6.25	6.25	50	25	36.3 $\pm$ 0.1	>200	6
VAN [ $\mu$ g mL <sup>-1</sup> ]	1	1	1	0.25	1	8			

<sup>a</sup> Antibacterial activity is displayed as MIC [ $\mu$ M]. MRSA – methicillin resistant *S. aureus*; MSSA – methicillin susceptible *S. aureus*; Se – *S. epidermidis*; Bs – *Bacillus subtilis*; En – *Enterococcus* spp En VRE – *Enterococcus casseliflavus* VRE, CC<sub>50</sub> – HuDe cells; HC<sub>50</sub> – human red blood cells; TI – therapeutic index, determined by dividing the lowest value between CC<sub>50</sub> and HC<sub>50</sub> with the lowest MIC value for each compound; VAN – vancomycin. MIC determined with  $n = 4$  across two biological replicates.

coupled with low haemolytic activity, cytotoxicity and high stability under biological conditions.

### Characterisation of CO-releasing properties of MnG9MeBeIm

Based on previous studies of manganese tricarbonyl complexes, the involvement of CO release in the antibacterial mode of action is a plausible hypothesis. To assess whether CO is involved in the antibacterial activity of our lead compound we re-measured the MIC of the compound against MRSA in the presence and absence of haemoglobin (Hb), a well-established CO-scavenger. Indeed, we observed a significant 4–8 $\times$  increase in MIC for **MnG9MeBeIm** in the presence of 20  $\mu$ M Hb. Next, we conducted a checkerboard assay varying both the concentrations of **MnG9MeBeIm** and Hb (Fig. 6A). A clear antagonistic (FICI  $\gg$  4)<sup>47</sup> effect of Hb on the antibacterial activity of **MnG9MeBeIm** was observed presumably by irreversibly binding the CO released by the manganese compound. However, even in the presence of large concentrations of Hb, the activity of **MnG9MeBeIm** was not completely inhibited, suggesting that multiple mechanisms may be involved (the MIC<sub>MnG8MeBeIm</sub> in the presence of 160  $\mu$ M Hb was 50  $\mu$ M). The release of CO was observed *via* UV/vis spectroscopy, monitoring the absorbance changes of Hb in the presence of **MnG9MeBeIm** over time. The conversion of deoxy-Hb to Hb-CO was observed over 8 h (25 °C) (Fig. 6B). These results combined with the structural similarity and the common MnCO<sub>3</sub> scaffold in our library suggest that CO-release is a factor in the antibacterial effect of all these compounds. However, the distinct levels of antibacterial activity observed across this library suggests that the structure of the compound has a significant effect on the characteristics of the CO release and possibly bacterial uptake which in turn affects their efficacy against bacteria.

### Bacterial cytological profiling of MnG9MeBeIm

To obtain a general assessment of the effect of **MnG9MeBeIm** on bacteria, we performed bacterial cytological profiling (BCP)

in *Bacillus subtilis*.<sup>48,49</sup> Growth curve experiments with different concentrations of the compound were conducted to determine the optimal amount and the ideal incubation time, which was found to be 3  $\mu$ M for 20 min. A *B. subtilis* strain with the *PrpsD-gfp* reporter was incubated with **MnG9MeBeIm** for 15 min before the DNA stain DAPI and the membrane stain Nile red were added, and the bacteria were imaged with a fluorescence microscope. No significant differences were observed in the GFP or DAPI images, while the Nile red staining was clearly different, showing multiple hotspots on the bacterial membrane (Fig. 7B). Indeed, slightly lower GFP signal is visible at these locations suggesting the presence of small invaginations. As **MnG9MeBeIm** seemed to have a distinct effect on the bacterial membrane, we incubated a MinD-GFP reporter with the compound to observe any effects on membrane polarisation.<sup>49</sup> MinD is involved in cell division regulation and localises at the bacterial cell poles and septa. Membrane depolarisation perturbs the MinD localisation significantly.<sup>50</sup> With our compound similar ‘blob-like’ accumulations as with the Nile red were observed. However, the pattern was distinctly different from the positive control nisin (Fig. 7B) where complete dispersal of MinD was observed, indicating that **MnG9MeBeIm** does not affect membrane polarisation but forms invaginations which might disturb MinD localisation. Finally, based on the results indicating that CO release is involved in the mode of action of the compound *B. subtilis* was incubated with both **MnG9MeBeIm** and COP-1, a fluorescent probe to detect intracellular CO, and the cells were stained with Nile red (Fig. 7C).<sup>51</sup> From the imaging at the COP-1 emission wavelength it is clear that CO is being released, which triggers the observed fluorescence. Additionally, the blobs observed with Nile red coincide with the peaks in COP-1 fluorescence, indicating that CO is preferentially released in and around the membrane, further supporting the hypothesis that **MnG9MeBeIm** seems to have a distinct effect on the latter.



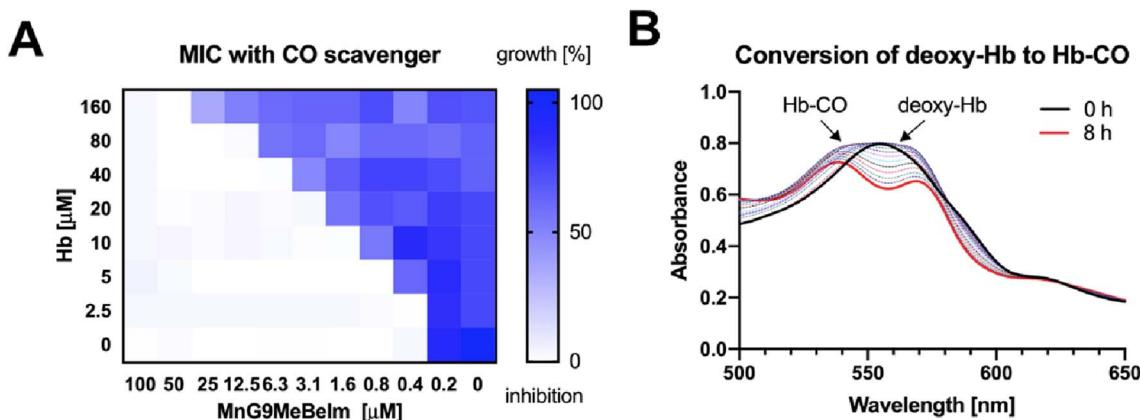


Fig. 6 Characterisation of CO-releasing behaviour of **MnG9MeBeIm**. (A) Checkerboard assay of the biological activity of the compound against MRSA displayed as growth percentage over the control, in the presence of different concentrations of the CO scavenger hemoglobin. (B) Conversion of deoxyhemoglobin (80  $\mu$ M, HEPES pH 7.4, 25 °C) to carboxyhemoglobin in the presence of **MnG9MeBeIm** (20  $\mu$ M) monitored over an 8 hours period.

### Effect of MnG9MeBeIm on the bacterial membrane

Based on the microscopy results, an effect of **MnG9MeBeIm** on the bacterial membrane seemed apparent. In previous work, some manganese tricarbonyl compounds were found to induce pore formation and other detrimental effects on the bacterial

membrane.<sup>23</sup> To investigate the effect of **MnG9MeBeIm** on the membrane, we utilised propidium iodide (PI), a fluorescent agent that is unable to traverse intact membranes but accumulates if the latter becomes compromised by pores. Comparison with sodium dodecyl sulfate (SDS), a surfactant known to

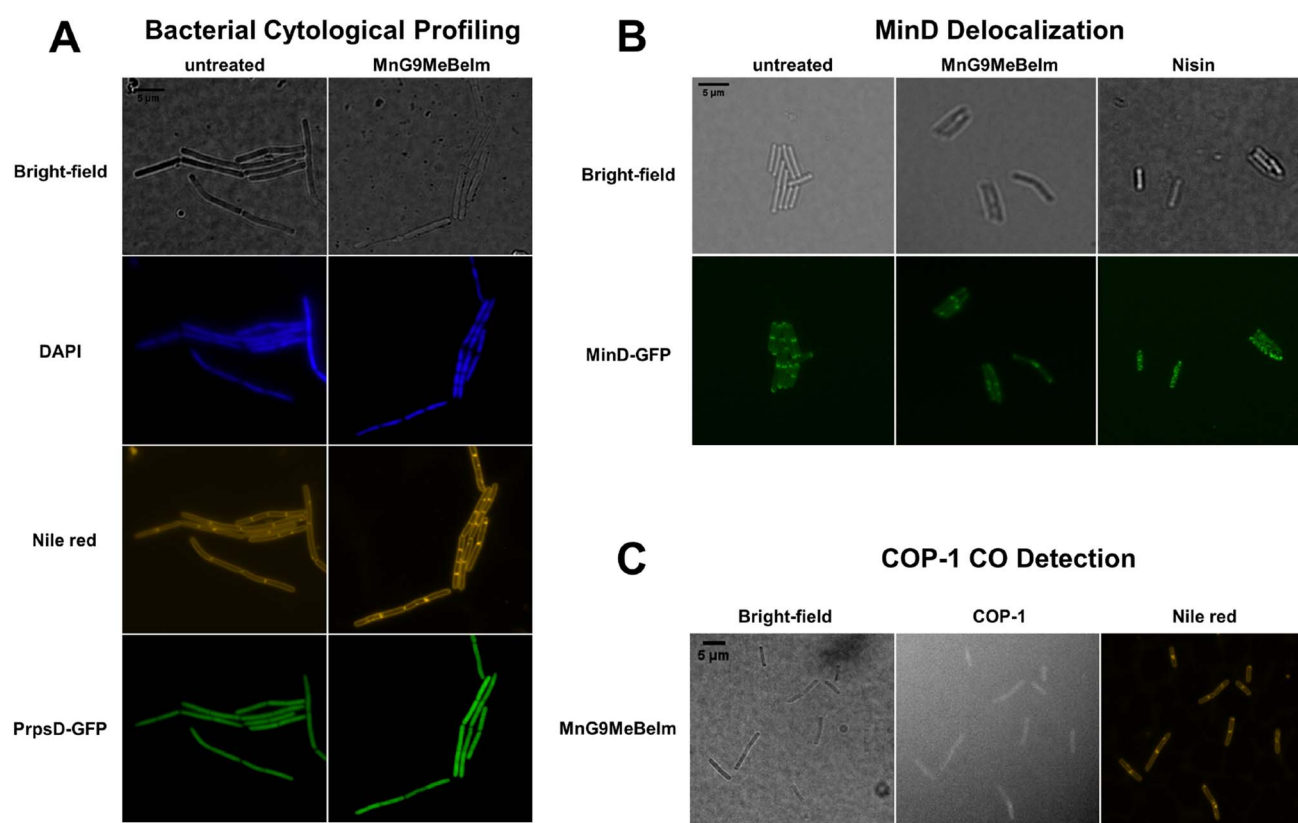


Fig. 7 Fluorescence microscopy pictures obtained. (A) BCP: *B. subtilis* *PrpsD* strain incubated with 6.25  $\mu$ M **MnG9MeBeIm** for 20 min and stained with DAPI (1  $\mu$ g  $\text{mL}^{-1}$ ) and Nile red (0.5  $\mu$ g  $\text{mL}^{-1}$ ) compared with untreated control. (B) *B. subtilis* with MinD reporter incubated with 6.25  $\mu$ M **MnG9MeBeIm** for 20 min compared with untreated control and nisin (100  $\mu$ g  $\text{mL}^{-1}$ ). (C) *B. subtilis* incubated with 6.25  $\mu$ M **MnG9MeBeIm** for 20 min in the presence of COP-1 (5  $\mu$ M) and stained with Nile red (0.5  $\mu$ g  $\text{mL}^{-1}$ ).

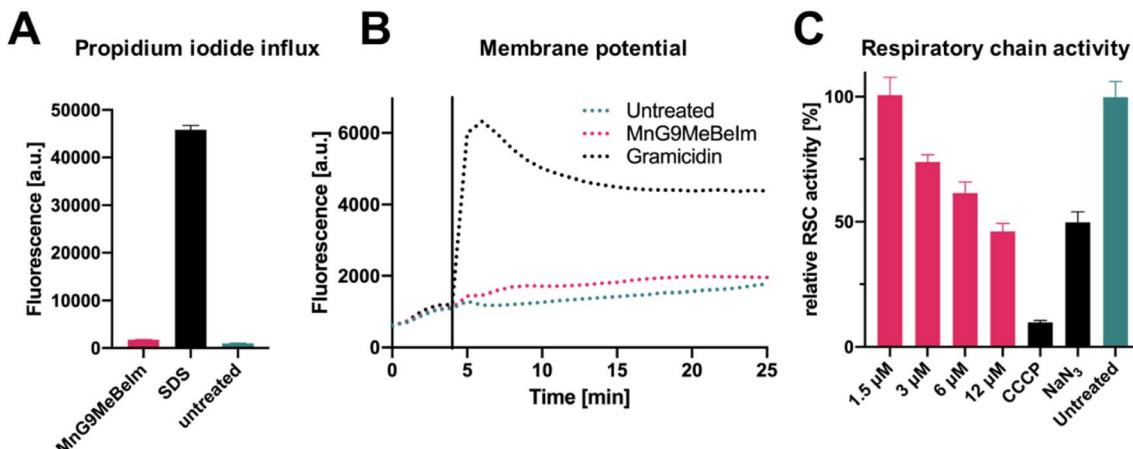


Fig. 8 Mode of action characterisation for **MnG9MeBelm**. (A) Quantified PI fluorescence in bacteria after exposure to **MnG9MeBelm** (3  $\mu$ M, 20 min), SDS (positive control, 0.05%, 20 min) or no compound. (B) DiOC<sub>2</sub> fluorescence as a measure of membrane depolarisation after addition of **MnG9MeBelm** (3  $\mu$ M), gramicidin (positive control 1  $\mu$ g mL<sup>-1</sup>). The straight black line indicates the time point of antibiotic addition. (C) Relative respiratory chain activity measured by resazurin reduction. **MnG9MeBelm** was tested at 4 concentrations (after 20 min incubation) and compared to the positive controls CCCP (100  $\mu$ M, 20 min) and NaN<sub>3</sub> (15 mM, 20 min).

form large pores in membranes, showed that **MnG9MeBelm** causes no significant uptake of PI into the bacteria (Fig. 8A). A DiOC<sub>2</sub> assay was performed to investigate any effects on membrane polarisation. The absence of any significant fluorescence increase caused by displacement of DiOC<sub>2</sub> from bacterial membranes is in agreement with the distinct MinD distribution pattern described earlier (Fig. 7B), suggesting **MnG9MeBelm** does not affect membrane polarisation. Together with the PI assay these experiments demonstrate that any effect the lead compound exerts on the bacterial membrane does not involve pore formation or depolarisation. In previous reports, the inhibition of the respiratory chain was implied as a target for a ruthenium-based CORM (of note, it has been questioned whether the antibacterial effect of Ru-CORMs is indeed due to CO-release).<sup>52,53</sup> To interrogate whether **MnG9MeBelm** affects the respiratory chain we quantified the respiratory activity by monitoring resazurin reduction.<sup>54</sup> A dose-dependent decrease in respiratory chain activity was observed (Fig. 8C), suggesting that the CO released by the compounds indeed inhibits the electron transport chain. The effect at the highest concentration tested was comparable to that of sodium azide, a well-known inhibitor of the electron transport chain (Fig. 8C).<sup>55</sup> Growth-curve experiments at the same concentrations showed that bacterial growth is not significantly inhibited at these concentrations and at these time-frames indicating that the observed resazurin reduction is likely due to respiratory chain inhibition (Fig. S18†). The aerobic respiratory chain is located in the plasma membrane of bacteria and hence the observation that **MnG9MeBelm** causes bacterial death by its inhibition coincides well with the fluorescent microscopy data discussed earlier.

## Conclusion

To accelerate the pace of discovery for novel metalloantibiotics we have applied combinatorial chemistry to the preparation of

manganese tricarbonyl compounds for the first time. This enabled the preparation and antibacterial screening of 420 new Schiff-base Mn(CO)<sub>3</sub> complexes. A large fraction of the compounds (64/420, 15.3%) showed significant activity against MRSA (MIC  $\leq$  12.5  $\mu$ M) and only inactive compounds displayed haemolysis against human red blood cells. Based on this crude screening data we selected 10 lead compounds, maximizing for activity and structural diversity. These compounds were resynthesised in batch, purified and fully characterised. Re-measuring of antibacterial activity and human cell toxicity revealed **MnG9MeBelm** as lead compound displaying a therapeutic index of over 100. X-ray diffraction unambiguously confirmed the structure of **MnG9MeBelm**. The CO-releasing properties of the complex were characterised, revealing a slow release of the CO-ligands. The presence of Hb reduces the antibacterial activity of the lead compound, implying a significant role of CO in its mode of bacterial killing. Mode of action studies utilising BCP indicate a distinct effect of **MnG9MeBelm** on the bacterial membrane. Common modes of membrane interference such as pore formation and membrane depolarisation could be excluded and we could show that CO is released *in vitro* and colocalises with apparent membrane invaginations. Lastly, we show that the compound inhibits the aerobic respiratory chain which is located in the bacterial membrane. With this data, the lead compound is primed for initial *in vivo* evaluations for toxicity and efficacy.

Altogether we have efficiently screened a library of 420 new metal compounds for their antibacterial properties. The observed hit-rate is in line and even exceeds that of previous screening initiatives.<sup>4,56</sup> The approach of directly screening crude reaction mixtures for antibacterial properties is vindicated by the excellent agreement of crude reaction results with the measurements conducted on the purified manganese complexes. Building on this approach and expanding it to other metal-scaffolds together with the automation of the reaction set-up will enable the preparation and screening of orders of



magnitude larger metal complex libraries in the near future, enabling a more efficient exploration of the metal complex space for promising new metalloantibiotics.

## Data availability

We have provided all relevant data in the ESI† of the paper.

## Author contributions

A. F conceived the project and designed the library of building blocks. M. S. conducted all the synthesis, characterisation and biological assays. M. P. B. conducted experiments and data evaluation for the revision of this manuscript. S. P. conducted the cytotoxicity studies. G. P. conducted the crystallographic analysis. A. F. and M. S. analyzed the data. A. F. composed the manuscript. All authors discussed, commented and approved the final manuscript.

## Conflicts of interest

There are no conflicts to declare.

## Acknowledgements

We thank Prof. Jean-Louis Reymond for generously hosting and supporting our research group. Prof. Michaela Wenzel and Ann-Britt Schäfer are acknowledged for their introduction to BCP and providing the GFP-fused *B. subtilis* strains. Prof. Cristina Bacci and Dr Martina Rega are acknowledged for the gift of clinical isolate bacteria strains. This work has benefited from the equipment and framework of the COMP-HUB and COMP-R Initiatives, funded by the 'Departments of Excellence' program of the Italian Ministry for University and Research (MIUR, 2018–2022 and MUR, 2023–2027) We also thank Prof. Christoph von Ballmoos and Nicola Dolder for access and introduction to their fluorescence microscope. We thank Çağrı Özsan for helpful comments and proofreading during the preparation of this manuscript. Acknowledgments to the University of Bern's crystallography support staff for their assistance, and to Chiesi Farmaceutici SpA and Dr Davide Balestri for their support with the D8 Venture X-ray equipment. A. F. gratefully acknowledges funding from the Swiss National Science Foundation Ambizione grant PZ00P2\_202016 and support by the University of Bern.

## References

- 1 C. J. Murray, K. S. Ikuta, F. Sharara, L. Swetschinski, G. R. Aguilar, A. Gray, C. Han, C. Bisignano, P. Rao, E. Wool, S. C. Johnson, A. J. Browne, M. G. Chipeta, F. Fell, S. Hackett, G. Haines-Woodhouse, B. H. K. Hamadani, E. A. P. Kumaran, B. McManigal, R. Agarwal, S. Akech, S. Albertson, J. Amuasi, J. Andrews, A. Aravkin, E. Ashley, F. Bailey, S. Baker, B. Basnyat, A. Bekker, R. Bender, A. Bethou, J. Bielicki, S. Boonkasidecha, J. Bukosia, C. Carvalheiro, C. Castañeda-Orjuela, V. Chansamouth,

S. Chaurasia, S. Chiurchiù, F. Chowdhury, A. J. Cook, B. Cooper, T. R. Cressey, E. Criollo-Mora, M. Cunningham, S. Darboe, N. P. J. Day, M. D. Luca, K. Dokova, A. Dramowski, S. J. Dunachie, T. Eckmanns, D. Eibach, A. Emami, N. Feasey, N. Fisher-Pearson, K. Forrest, D. Garrett, P. Gastmeier, A. Z. Giref, R. C. Greer, V. Gupta, S. Haller, A. Haselbeck, S. I. Hay, M. Holm, S. Hopkins, K. C. Iregbu, J. Jacobs, D. Jarovsky, F. Javanmardi, M. Khorana, N. Kissoon, E. Kobeissi, T. Kostyanev, F. Krapp, R. Krumkamp, A. Kumar, H. H. Kyu, C. Lim, D. Limmathurotsakul, M. J. Loftus, M. Lunn, J. Ma, N. Mturi, T. Munera-Huertas, P. Musicha, M. M. Mussi-Pinhata, T. Nakamura, R. Nanavati, S. Nangia, P. Newton, C. Ngoun, A. Novotney, D. Nwakanma, C. W. Obiero, A. Olivas-Martinez, P. Olliaro, E. Ooko, E. Ortiz-Brizuela, A. Y. Peleg, C. Perrone, N. Plakkal, A. Ponce-de-Leon, M. Raad, T. Ramdin, A. Riddell, T. Roberts, J. V. Robotham, A. Roca, K. E. Rudd, N. Russell, J. Schnall, J. A. G. Scott, M. Shivamallappa, J. Sifuentes-Osornio, N. Steenkeste, A. J. Stewardson, T. Stoeva, N. Tasak, A. Thaiprakong, G. Thwaites, C. Turner, P. Turner, H. R. van Doorn, S. Velaphi, A. Vongpradith, H. Vu, T. Walsh, S. Waner, T. Wangrangsimakul, T. Wozniak, P. Zheng, B. Sartorius, A. D. Lopez, A. Stergachis, C. Moore, C. Dolecek and M. Naghavi, Global Burden of Bacterial Antimicrobial Resistance in 2019: A Systematic Analysis, *Lancet*, 2022, **399**(10325), 629–655, DOI: [10.1016/S0140-6736\(21\)02724-0](https://doi.org/10.1016/S0140-6736(21)02724-0).

2 M. S. Butler, I. R. Henderson, R. J. Capon and M. A. T. Blaskovich, Antibiotics in the Clinical Pipeline as of December 2022, *J. Antibiot.*, 2023, **76**(8), 431–473, DOI: [10.1038/s41429-023-00629-8](https://doi.org/10.1038/s41429-023-00629-8).

3 V. Bhandari and A. Suresh, Next-Generation Approaches Needed to Tackle Antimicrobial Resistance for the Development of Novel Therapies Against the Deadly Pathogens, *Front. Pharmacol.*, 2022, **13**, DOI: [10.3389/fphar.2022.838092](https://doi.org/10.3389/fphar.2022.838092).

4 A. Frei, J. Zuegg, A. G. Elliott, M. Baker, S. Braese, C. Brown, F. Chen, C. G. Dowson, G. Dujardin, N. Jung, A. P. King, A. M. Mansour, M. Massi, J. Moat, H. A. Mohamed, A. K. Renfrew, P. J. Rutledge, P. J. Sadler, M. H. Todd, C. E. Willans, J. J. Wilson, M. A. Cooper and M. A. T. Blaskovich, Metal Complexes as a Promising Source for New Antibiotics, *Chem. Sci.*, 2020, **11**, 2627–2639, DOI: [10.1039/C9SC06460E](https://doi.org/10.1039/C9SC06460E).

5 K. L. Smitten, H. M. Southam, J. B. de la Serna, M. R. Gill, P. J. Jarman, C. G. W. Smythe, R. K. Poole and J. A. Thomas, Using Nanoscopy To Probe the Biological Activity of Antimicrobial Leads That Display Potent Activity against Pathogenic, Multidrug Resistant, Gram-Negative Bacteria, *ACS Nano*, 2019, **13**(5), 5133–5146, DOI: [10.1021/acsnano.8b08440](https://doi.org/10.1021/acsnano.8b08440).

6 K. L. Smitten, S. D. Fairbanks, C. C. Robertson, J. B. de la Serna, S. J. Foster and J. A. Thomas, Ruthenium Based Antimicrobial Theranostics—Using Nanoscopy to Identify Therapeutic Targets and Resistance Mechanisms in



Staphylococcus Aureus, *Chem. Sci.*, 2019, **11**(1), 70–79, DOI: [10.1039/C9SC04710G](https://doi.org/10.1039/C9SC04710G).

7 K. Smitten, H. M. Southam, S. Fairbanks, A. Graf, A. Chauvet and J. A. Thomas, Clearing an ESKAPE Pathogen in a Model Organism; a Polypyridyl Ruthenium(II) Complex Theranostic That Treats a Resistant Acinetobacter Baumannii Infection in *Galleria Mellonella*, *Chem.–Eur. J.*, 2023, **29**, e202203555, DOI: [10.1002/chem.202203555](https://doi.org/10.1002/chem.202203555).

8 F. Li, J. G. Collins and F. R. Keene, Ruthenium Complexes as Antimicrobial Agents, *Chem. Soc. Rev.*, 2015, **44**(8), 2529–2542, DOI: [10.1039/C4CS00343H](https://doi.org/10.1039/C4CS00343H).

9 A. Frei, Metal Complexes, an Untapped Source of Antibiotic Potential?, *Antibiotics*, 2020, **9**, 90, DOI: [10.3390/antibiotics9020090](https://doi.org/10.3390/antibiotics9020090).

10 F. Li, E. J. Harry, A. L. Bottomley, M. D. Edstein, G. W. Birrell, C. E. Woodward, F. R. Keene and J. G. Collins, Dinuclear Ruthenium(II) Antimicrobial Agents That Selectively Target Polysomes in Vivo, *Chem. Sci.*, 2013, **5**(2), 685–693, DOI: [10.1039/C3SC52166D](https://doi.org/10.1039/C3SC52166D).

11 F. Li, M. Feterl, Y. Mulyana, J. M. Warner, J. G. Collins and F. R. Keene, Vitro Susceptibility and Cellular Uptake for a New Class of Antimicrobial Agents: Dinuclear Ruthenium(II) Complexes, *J. Antimicrob. Chemother.*, 2012, **67**(11), 2686–2695, DOI: [10.1093/jac/dks291](https://doi.org/10.1093/jac/dks291).

12 D. K. Weber, M.-A. Sani, M. T. Downton, F. Separovic, F. R. Keene and J. G. Collins, Membrane Insertion of a Dinuclear Polypyridylruthenium(II) Complex Revealed by Solid-State NMR and Molecular Dynamics Simulation: Implications for Selective Antibacterial Activity, *J. Am. Chem. Soc.*, 2016, **138**(46), 15267–15277, DOI: [10.1021/jacs.6b09996](https://doi.org/10.1021/jacs.6b09996).

13 M. Patra, M. Wenzel, P. Prochnow, V. Pierroz, G. Gasser, J. E. Bandow and N. Metzler-Nolte, An Organometallic Structure-Activity Relationship Study Reveals the Essential Role of a Re(CO)<sub>3</sub> Moiety in the Activity against Gram-Positive Pathogens Including MRSA, *Chem. Sci.*, 2014, **6**(1), 214–224, DOI: [10.1039/C4SC02709D](https://doi.org/10.1039/C4SC02709D).

14 A. Frei, M. Amado, M. A. Cooper and M. A. T. Blaskovich, Light-Activated Rhenium Complexes with Dual Mode of Action against Bacteria 10.1002/chem.201904689, *Chem.–Eur. J.*, 2020, **26**, 2852, DOI: [10.1002/chem.201904689](https://doi.org/10.1002/chem.201904689).

15 S. N. Sovari, N. Radakovic, P. Roch, A. Crochet, A. Pavic, F. Zobi and A. M. R. Combatting, A Molecular Approach to the Discovery of Potent and Non-Toxic Rhenium Complexes Active against C. Albicans-MRSA Co-Infection, *Eur. J. Med. Chem.*, 2021, **226**, 113858, DOI: [10.1016/j.ejmech.2021.113858](https://doi.org/10.1016/j.ejmech.2021.113858).

16 S. N. Sovari, S. Vojnovic, S. S. Bogojevic, A. Crochet, A. Pavic, J. Nikodinovic-Runic and F. Zobi, Design, Synthesis and *in Vivo* Evaluation of 3-Arylcoumarin Derivatives of Rhenium(I) Tricarbonyl Complexes as Potent Antibacterial Agents against Methicillin-Resistant Staphylococcus Aureus (MRSA), *Eur. J. Med. Chem.*, 2020, **205**, 112533, DOI: [10.1016/j.ejmech.2020.112533](https://doi.org/10.1016/j.ejmech.2020.112533).

17 S. S. Mendes, J. Marques, E. Mesterházy, J. Straetener, M. Arts, T. Pissarro, J. Reginold, A. Berscheid, J. Bornikoel, R. M. Kluj, C. Mayer, F. Oesterhelt, S. Friäes, B. Royo, T. Schneider, H. Brötz-Oesterhelt, C. C. Romão and L. M. Saraiva, Synergetic Antimicrobial Activity and Mechanism of Clotrimazole-Linked CO-Releasing Molecules, *ACS Bio Med Chem Au*, 2022, **2**(4), 419–436, DOI: [10.1021/acsbiomedchemau.2c00007](https://doi.org/10.1021/acsbiomedchemau.2c00007).

18 C. Nagel, S. McLean, R. K. Poole, H. Braunschweig, T. Kramer and U. Schatzschneider, Introducing [Mn(CO)<sub>3</sub>(Tpa- $\kappa$ 3N)]<sup>+</sup> as a Novel Photoactivatable CO-Releasing Molecule with Well-Defined iCORM Intermediates–Synthesis, Spectroscopy, and Antibacterial Activity, *Dalton Trans.*, 2014, **43**(26), 9986–9997, DOI: [10.1039/C3DT51848E](https://doi.org/10.1039/C3DT51848E).

19 J. Betts, C. Nagel, U. Schatzschneider, R. Poole and R. M. L. Ragione, Antimicrobial Activity of Carbon Monoxide-Releasing Molecule [Mn(CO)<sub>3</sub>(Tpa- $\kappa$ 3N)]Br *versus* Multidrug-Resistant Isolates of Avian Pathogenic Escherichia Coli and Its Synergy with Colistin, *PLoS One*, 2017, **12**(10), e0186359, DOI: [10.1371/journal.pone.0186359](https://doi.org/10.1371/journal.pone.0186359).

20 N. Rana, H. E. Jesse, M. Tinajero-Trejo, J. A. Butler, J. D. Tarlit, M. L. von und zur Muhlen, C. Nagel, U. Schatzschneider and R. K. Poole, A Manganese Photosensitive Tricarbonyl Molecule [Mn(CO)<sub>3</sub>(Tpa- $\kappa$ 3N)]Br Enhances Antibiotic Efficacy in a Multi-Drug-Resistant Escherichia Coli, *Microbiology*, 2017, **163**(10), 1477–1489, DOI: [10.1099/mic.0.000526](https://doi.org/10.1099/mic.0.000526).

21 M. Tinajero-Trejo, N. Rana, C. Nagel, H. E. Jesse, T. W. Smith, L. K. Wareham, M. Hippler, U. Schatzschneider and R. K. Poole, Antimicrobial Activity of the Manganese Photoactivated Carbon Monoxide-Releasing Molecule [Mn(CO)<sub>3</sub>(Tpa- $\kappa$ 3N)]<sup>+</sup> Against a Pathogenic Escherichia Coli That Causes Urinary Infections, *Antioxid. Redox Signaling*, 2016, **24**(14), 765–780, DOI: [10.1089/ars.2015.6484](https://doi.org/10.1089/ars.2015.6484).

22 P. V. Simpson, C. Nagel, H. Bruhn and U. Schatzschneider, Antibacterial and Antiparasitic Activity of Manganese(I) Tricarbonyl Complexes with Ketoconazole, Miconazole, and Clotrimazole Ligands, *Organometallics*, 2015, **34**(15), 3809–3815, DOI: [10.1021/acs.organomet.5b00458](https://doi.org/10.1021/acs.organomet.5b00458).

23 P. Güntzel, C. Nagel, J. Weigelt, J. W. Betts, C. A. Patrick, H. M. Southam, R. M. La Ragione, R. K. Poole and U. Schatzschneider, Biological Activity of Manganese(I) Tricarbonyl Complexes on Multidrug-Resistant Gram-Negative Bacteria: From Functional Studies to *in Vivo* Activity in *Galleria Mellonella*, *Metallomics*, 2019, **11**(12), 2033–2042, DOI: [10.1039/c9mt00224c](https://doi.org/10.1039/c9mt00224c).

24 J. W. Betts, P. Roth, C. A. Patrick, H. M. Southam, R. M. La Ragione, R. K. Poole and U. Schatzschneider, Antibacterial Activity of Mn(I) and Re(I) Tricarbonyl Complexes Conjugated to a Bile Acid Carrier Molecule, *Metallomics*, 2020, **12**(10), 1563–1575, DOI: [10.1039/d0mt00142b](https://doi.org/10.1039/d0mt00142b).

25 J. W. Betts, S. Cawthraw, J. A. Smyth, R. K. Poole, P. Roth, U. Schatzschneider and R. M. La Ragione, The Manganese Carbonyl Complex [Mn(CO)<sub>3</sub>(Tqa- $\kappa$ 3N)]Br: A Novel Antimicrobial Agent with the Potential to Treat Avian Pathogenic Escherichia Coli (APEC) Infections, *Vet. Microbiol.*, 2023, **284**, 109819, DOI: [10.1016/j.vetmic.2023.109819](https://doi.org/10.1016/j.vetmic.2023.109819).



26 J. S. Ward, J. M. Lynam, J. Moir and I. J. S. Fairlamb, Visible-Light-Induced CO Release from a Therapeutically Viable Tryptophan-Derived Manganese(I) Carbonyl (TryptoCORM) Exhibiting Potent Inhibition against *E. coli*, *Chem.-Eur. J.*, 2014, **20**(46), 15061–15068, DOI: [10.1002/chem.201403305](https://doi.org/10.1002/chem.201403305).

27 J. S. Ward, R. Morgan, J. M. Lynam, I. J. S. Fairlamb and J. W. B. Moir, Toxicity of Tryptophan Manganese(I) Carbonyl (Trypto-CORM), against *Neisseria Gonorrhoeae*, *MedChemComm*, 2017, **8**(2), 346–352, DOI: [10.1039/C6MD00603E](https://doi.org/10.1039/C6MD00603E).

28 S. H. Crook, B. E. Mann, A. J. H. M. Meijer, H. Adams, P. Sawle, D. Scapens and R. Motterlini,  $[\text{Mn}(\text{CO})_4 \{S_2\text{CNMe}(\text{CH}_2\text{CO}_2\text{H})\}]$ , a New Water-Soluble CO-Releasing Molecule, *Dalton Trans.*, 2011, **40**(16), 4230–4235, DOI: [10.1039/C1DT10125K](https://doi.org/10.1039/C1DT10125K).

29 L. K. Wareham, S. McLean, R. Begg, N. Rana, S. Ali, J. J. Kendall, G. Sanguinetti, B. E. Mann and R. K. Poole, The Broad-Spectrum Antimicrobial Potential of  $[\text{Mn}(\text{CO})_4 \{S_2\text{CNMe}(\text{CH}_2\text{CO}_2\text{H})\}]$ , a Water-Soluble CO-Releasing Molecule (CORM-401): Intracellular Accumulation, Transcriptomic and Statistical Analyses, and Membrane Polarization, *Antioxid. Redox Signaling*, 2018, **28**(14), 1286–1308, DOI: [10.1089/ars.2017.7239](https://doi.org/10.1089/ars.2017.7239).

30 R. Liu, X. Li and K. S. Lam, Combinatorial Chemistry in Drug Discovery, *Curr. Opin. Chem. Biol.*, 2017, **38**, 117–126, DOI: [10.1016/j.cbpa.2017.03.017](https://doi.org/10.1016/j.cbpa.2017.03.017).

31 N. Favalli, G. Bassi, J. Scheuermann and D. Neri, DNA-Encoded Chemical Libraries—Achievements and Remaining Challenges, *FEBS Lett.*, 2018, **592**(12), 2168–2180, DOI: [10.1002/1873-3468.13068](https://doi.org/10.1002/1873-3468.13068).

32 M. S. Lowry, W. R. Hudson, R. A. Pascal and S. Bernhard, Accelerated Luminophore Discovery through Combinatorial Synthesis, *J. Am. Chem. Soc.*, 2004, **126**(43), 14129–14135, DOI: [10.1021/ja047156+](https://doi.org/10.1021/ja047156+).

33 V. Mdluli, S. Diluzio, J. Lewis, J. F. Kowalewski, T. U. Connell, D. Yaron, T. Kowalewski and S. Bernhard, High-Throughput Synthesis and Screening of Iridium(III) Photocatalysts for the Fast and Chemoselective Dehalogenation of Aryl Bromides, *ACS Catal.*, 2020, **10**(13), 6977–6987, DOI: [10.1021/acscatal.0c02247](https://doi.org/10.1021/acscatal.0c02247).

34 S. DiLuzio, V. Mdluli, T. U. Connell, J. Lewis, V. VanBenschoten and S. Bernhard, High-Throughput Screening and Automated Data-Driven Analysis of the Triplet Photophysical Properties of Structurally Diverse, Heteroleptic Iridium(III) Complexes, *J. Am. Chem. Soc.*, 2021, **143**(2), 1179–1194, DOI: [10.1021/jacs.0c12290](https://doi.org/10.1021/jacs.0c12290).

35 T. Zach, F. Geyer, B. Kiendl, J. Mößeler, O. Nguyen, T. Schmidpeter, P. Schuster, C. Nagel and U. Schatzschneider, Electrospray Mass Spectrometry to Study Combinatorial iClick Reactions and Multiplexed Kinetics of  $[\text{Ru}(\text{N}_3)(\text{N}^{\wedge}\text{N})(\text{Terpy})]\text{PF}_6$  with Alkynes of Different Steric and Electronic Demand, *Inorg. Chem.*, 2023, **62**(7), 2982–2993, DOI: [10.1021/acs.inorgchem.2c03377](https://doi.org/10.1021/acs.inorgchem.2c03377).

36 M. J. Chow, C. Licona, D. Yuan Qiang Wong, G. Pastorin, C. Gaiddon and W. H. Ang, Discovery and Investigation of Anticancer Ruthenium–Arene Schiff-Base Complexes via Water-Promoted Combinatorial Three-Component Assembly, *J. Med. Chem.*, 2014, **57**(14), 6043–6059, DOI: [10.1021/jm500455p](https://doi.org/10.1021/jm500455p).

37 M. Juinn Chow, M. Alfiean, G. Pastorin, C. Gaiddon and W. Han Ang, Apoptosis-Independent Organoruthenium Anticancer Complexes That Overcome Multidrug Resistance: Self-Assembly and Phenotypic Screening Strategies, *Chem. Sci.*, 2017, **8**(5), 3641–3649, DOI: [10.1039/C7SC00497D](https://doi.org/10.1039/C7SC00497D).

38 C. Weng, L. Shen and W. H. Ang, Harnessing Endogenous Formate for Antibacterial Prodrug Activation by in Cellulo Ruthenium-Mediated Transfer Hydrogenation Reaction, *Angew. Chem., Int. Ed.*, 2020, **59**(24), 9314–9318, DOI: [10.1002/anie.202000173](https://doi.org/10.1002/anie.202000173).

39 C. Weng, L. Shen, J. W. Teo, Z. C. Lim, B. S. Loh and W. H. Ang, Targeted Antibacterial Strategy Based on Reactive Oxygen Species Generated from Dioxigen Reduction Using an Organoruthenium Complex, *JACS Au*, 2021, **1**(9), 1348–1354, DOI: [10.1021/jacsau.1c00262](https://doi.org/10.1021/jacsau.1c00262).

40 C. Weng, H. Yang, B. S. Loh, M. W. Wong and W. H. Ang, Targeting Pathogenic Formate-Dependent Bacteria with a Bioinspired Metallo–Nitroreductase Complex, *J. Am. Chem. Soc.*, 2023, **145**(11), 6453–6461, DOI: [10.1021/jacs.3c00237](https://doi.org/10.1021/jacs.3c00237).

41 C. C. Konkankit, B. A. Vaughn, S. N. MacMillan, E. Boros and J. J. Wilson, Combinatorial Synthesis to Identify a Potent, Necrosis-Inducing Rhenium Anticancer Agent, *Inorg. Chem.*, 2019, **58**(6), 3895–3909, DOI: [10.1021/acs.inorgchem.8b03552](https://doi.org/10.1021/acs.inorgchem.8b03552).

42 C. C. Konkankit, B. A. Vaughn, Z. Huang, E. Boros and J. J. Wilson, Systematically Altering the Lipophilicity of Rhenium(I) Tricarbonyl Anticancer Agents to Tune the Rate at Which They Induce Cell Death, *Dalton Trans.*, 2020, **49**(45), 16062–16066, DOI: [10.1039/D0DT01097A](https://doi.org/10.1039/D0DT01097A).

43 R. Vilar, T. Kench, A. Rahardjo, A. Bellamkonda, T. E. Maher and M. Storch, A Semi-Automated, High-Throughput Approach for the Synthesis and Identification of Highly Photo-Cytotoxic Iridium Complexes, *ChemRxiv*, 2023, preprint, DOI: [10.26434/chemrxiv-2023-rt8kr](https://doi.org/10.26434/chemrxiv-2023-rt8kr).

44 D. Bajusz, A. Rácz and K. Héberger, Why Is Tanimoto Index an Appropriate Choice for Fingerprint-Based Similarity Calculations?, *J. Cheminf.*, 2015, **7**(1), 20, DOI: [10.1186/s13321-015-0069-3](https://doi.org/10.1186/s13321-015-0069-3).

45 Y. Cortat, M. Nedyalkova, K. Schindler, P. Kadakia, G. Demirci, S. Nasiri Sovari, A. Crochet, S. Salentinig, M. Lattuada, O. M. Steiner and F. Zobi, Computer-Aided Drug Design and Synthesis of Rhenium Clotrimazole Antimicrobial Agents, *Antibiotics*, 2023, **12**(3), 619, DOI: [10.3390/antibiotics12030619](https://doi.org/10.3390/antibiotics12030619).

46 A. G. Orpen, L. Brammer, F. H. Allen, O. Kennard, D. G. Watson and R. Taylor, Supplement. Tables of Bond Lengths Determined by X-Ray and Neutron Diffraction. Part 2. Organometallic Compounds and Co-Ordination Complexes of the d- and f-Block Metals, *J. Chem. Soc., Dalton Trans.*, 1989, **12**, S1–S83, DOI: [10.1039/DT98900000S1](https://doi.org/10.1039/DT98900000S1).



47 R. Huang, L. Pei, Q. Liu, S. Chen, H. Dou, G. Shu, Z. Yuan, J. Lin, G. Peng, W. Zhang and H. Fu, Isobologram Analysis: A Comprehensive Review of Methodology and Current Research, *Front. Pharmacol.*, 2019, **10**, DOI: [10.3389/fphar.2019.01222](https://doi.org/10.3389/fphar.2019.01222).

48 P. Nonejuie, M. Burkart, K. Pogliano and J. Pogliano, Bacterial Cytological Profiling Rapidly Identifies the Cellular Pathways Targeted by Antibacterial Molecules, *Proc. Natl. Acad. Sci. U. S. A.*, 2013, **110**(40), 16169–16174, DOI: [10.1073/pnas.1311066110](https://doi.org/10.1073/pnas.1311066110).

49 A.-B. Schäfer and M. Wenzel, A How-To Guide for Mode of Action Analysis of Antimicrobial Peptides, *Front. Cell. Infect. Microbiol.*, 2020, **10**, DOI: [10.3389/fcimb.2020.540898](https://doi.org/10.3389/fcimb.2020.540898).

50 H. Strahl and L. W. Hamoen, Membrane Potential Is Important for Bacterial Cell Division, *Proc. Natl. Acad. Sci. U. S. A.*, 2010, **107**(27), 12281–12286, DOI: [10.1073/pnas.1005485107](https://doi.org/10.1073/pnas.1005485107).

51 B. W. Michel, A. R. Lippert and C. J. Chang, A Reaction-Based Fluorescent Probe for Selective Imaging of Carbon Monoxide in Living Cells Using a Palladium-Mediated Carbonylation, *J. Am. Chem. Soc.*, 2012, **134**(38), 15668–15671, DOI: [10.1021/ja307017b](https://doi.org/10.1021/ja307017b).

52 A. M. Mansour, R. M. Khaled, E. Khaled, S. K. Ahmed, O. S. Ismael, A. Zeinhom, H. Magdy, S. S. Ibrahim and M. Abdelfatah, Ruthenium(II) Carbon Monoxide Releasing Molecules: Structural Perspective, Antimicrobial and Anti-Inflammatory Properties, *Biochem. Pharmacol.*, 2022, **199**, 114991, DOI: [10.1016/j.bcp.2022.114991](https://doi.org/10.1016/j.bcp.2022.114991).

53 V. G. Nielsen, Ruthenium, Not Carbon Monoxide, Inhibits the Procoagulant Activity of Atheris, Echis, and Pseudonaja Venoms, *Int. J. Mol. Sci.*, 2020, **21**(8), 2970, DOI: [10.3390/ijms21082970](https://doi.org/10.3390/ijms21082970).

54 D. Saeloh, V. Tipmanee, K. K. Jim, M. P. Dekker, W. Bitter, S. P. Voravuthikunchai, M. Wenzel and L. W. Hamoen, The Novel Antibiotic Rhodomyrtone Traps Membrane Proteins in Vesicles with Increased Fluidity, *PLoS Pathog.*, 2018, **14**(2), e1006876, DOI: [10.1371/journal.ppat.1006876](https://doi.org/10.1371/journal.ppat.1006876).

55 M. Tsubaki and S. Yoshikawa, Fourier-Transform Infrared Study of Azide Binding to the Fea3-CuB Binuclear Site of Bovine Heart Cytochrome c Oxidase: New Evidence for a Redox-Linked Conformational Change at the Binuclear Site, *Biochemistry*, 1993, **32**(1), 174–182, DOI: [10.1021/bi00052a023](https://doi.org/10.1021/bi00052a023).

56 A. Frei, A. G. Elliott, A. Kan, H. Dinh, S. Bräse, A. E. Bruce, M. R. Bruce, F. Chen, D. Humaidy, N. Jung, A. P. King, P. G. Lye, H. K. Maliszewska, A. M. Mansour, D. Matiadis, M. P. Muñoz, T.-Y. Pai, S. Pokhrel, P. J. Sadler, M. Sagnou, M. Taylor, J. J. Wilson, D. Woods, J. Zuegg, W. Meyer, A. K. Cain, M. A. Cooper and M. A. T. Blaskovich, Metal Complexes as Antifungals? From a Crowd-Sourced Compound Library to the First *In Vivo* Experiments, *JACS Au*, 2022, **2**(10), 2277–2294, DOI: [10.1021/jacsau.2c00308](https://doi.org/10.1021/jacsau.2c00308).

